Key Engineering Materials
ISSN: 1662-9795, Vol. 926, pp 1000-1006
doi:10.4028/p-bx41h4

Submitted: 2021-12-08
Revised: 2022-01-26
Accepted: 2022-02-04
Online: 2022-07-22

DIC Strain Monitoring during Fatigue of Cold-Formed High Strength Steel

Sanjay Gothivarekar[1,a], Albert Van Bael[1,b], Reza Talemi[1,c] and Sam Coppieters[1,d]

[1]Department of Materials Engineering, KU Leuven, 3001 Leuven, Belgium

[a]sanjay.gothivarekar@kuleuven.be, [b]albert.vanbael@kuleuven.be, [c]reza.talemi@kuleuven.be, [d]sam.coppieters@kuleuven.be

Keywords: Digital Image Correlation, Cold-forming, Fatigue, High strength steel

Abstract. Owing to the progressive use of cold-formed high strength steel (HSS) for transportation applications, a characterisation of the fatigue behaviour of HSS has become a focal point for material scientists and design engineers. To mimic the behaviour of cold-formed components, a specimen was adopted from previous research that features multiple bent sections. The geometry was obtained by consecutive bending operations at room temperature. When subsequent tensile cyclic loading is applied to the specimen, the localised damage from forming and stress concentrations cause crack initiation on the inside of the bent area. To investigate the effect of cold-forming on the fatigue behaviour experimentally, the evolution of the strain, displacement or stiffness can be monitored during fatigue testing. The current paper presents an experimental framework for investigating the strain fields of a bent specimen during fatigue. The evolution of the strain fields is then linked with characteristic fatigue mechanisms, such as crack initiation and growth.

Introduction

Structural components for mobile applications make use of a variety of HSS grades in different hollow shapes that require a specific forming operation. Since secondary forming is known to induce a considerable amount of residual stress, the resulting fatigue performance can be affected [1]. In that sense, an adapted specimen geometry and strain monitoring procedure can help to improve the understanding of the fatigue mechanism of a cold-formed part. Typically, fatigue crack initiation occurs in a gradual and often imperceptible way. This initiation period lasts until a pragmatically chosen critical crack length is reached [1]. Hereafter, fatigue crack propagation starts, that is characterised by an accelerated, exponential growth. Although a clear definition of these two periods exists, it is often challenging to detect the actual onset of crack propagation. For this reason, several experimental methods [2, 3] have been developed that are based on the degradation in strength of a fatigue specimen during testing. The first method investigates the evolution of the axial displacement of the fatigue specimen, measured by the fatigue bench crosshead [2]. The propagation threshold can then be linked to the exponential increase in displacement. The second method considers the evolution of the dynamic stiffness that is derived from the axial displacement and can be defined as ratio of deformation to the applied cyclic loading range [4]. In a more recent study on the fatigue behaviour of cold-formed HSS [2], an IR camera for lock-in thermography was used to monitor the temperature evolution of a fatigue specimen. To prove the applicability of these methods, microscopy was performed of a specimen of which the fatigue test was stopped at the pre-defined threshold. The observation of a micro-crack close to the critical crack length established the validity of these methods. In the current study, the feasibility of full-field strain measurements during fatigue is studied. Here, a stereo DIC set-up is used to monitor the area of crack initiation of a cold-formed HSS specimen. In addition, a microscopic analysis is included to shed a light on the characteristic fatigue fracture mode for the current HSS grade.

Materials and Specimen Design

A cold-formed specimen made of 5 mm thick S900MC HSS, is integrated in an experimental fatigue testing framework. This structural ('S') grade with minimum guaranteed yield strength of 900 MPa is produced through a thermo-mechanically controlled rolling process ('M'), is suitable for cold-forming ('C') and is in compliance with EN 10149-2 [5]. The corresponding microstructure o is shown in Fig. 1 a), where the lighter α-phase represents ferrite and β corresponds with banded martensite formations. From tensile testing, a yield strength $R_{p0.2\%}$ of 985 MPa, ultimate tensile strength R_m of 1095.5 MPa and maximum uniform strain ε_{max} of 0.136 are found, listed in Table 1.

Design engineers capitalise on the formability of the high strength metallic materials by progressively implementing them in cold-formed sections of load-carrying applications. Bending is considered to be a dominant forming operation and it is known that an adequate dimensioning and selection of bending tools is important for optimising the performance of the resulting bent component [6, 7]. Intuitively, a sufficiently large bend ratio (r/t), or ratio between the punch radius r and plate thickness t, can be chosen as this induces a lower residual stress in the bend. However, from a design point-of-view, smaller bend ratios are more interesting for obtaining compact bends.

In the current study, a specimen with several bent sections, shown in Fig. 1, is adopted to characterise the fatigue behaviour of bent HSS. In total three specimens are tested that were bent using three bend ratios (2, 2.5 and 3). For further details on the design, production and features of this specimen, the reader can consult previous studies [8, 9].

Table 1 Material properties of S900MC with thickness of 5 mm.

Direction	$R_{p0.2\%}$ (MPa)	R_m (MPa)	ε_{max}
RD-Avg.	985.2	1095.5	0.136

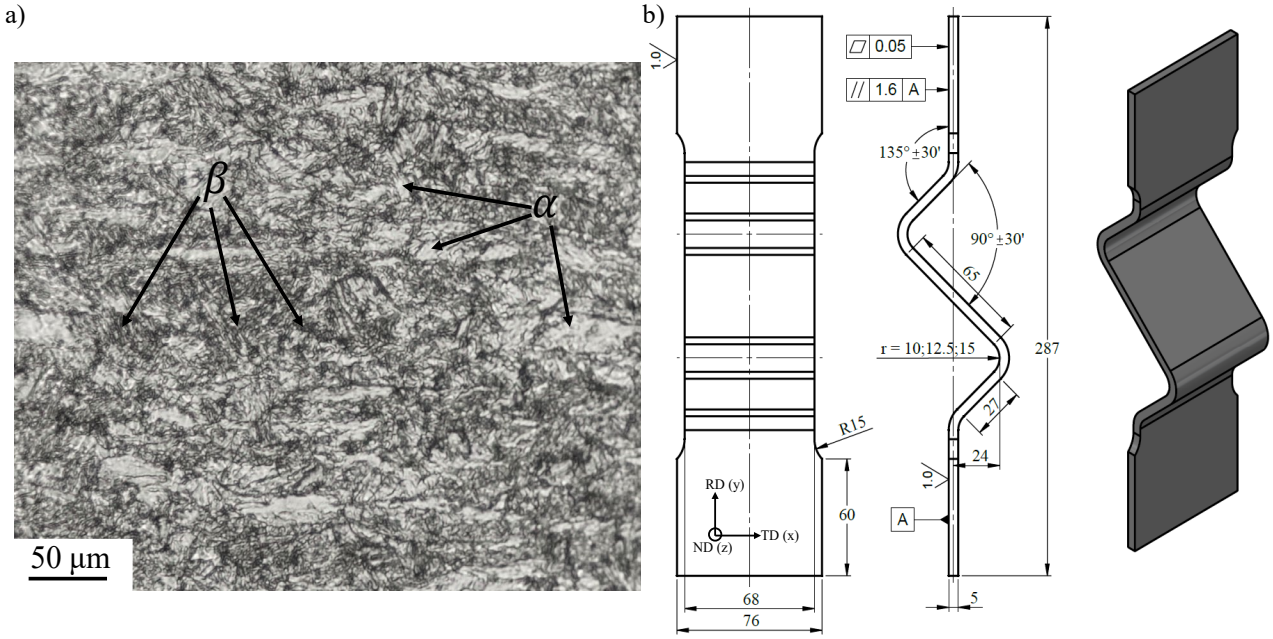

Figure 1 (a) Microstructure of S900MC. (b) Design of cold-formed fatigue specimen.

Fatigue Testing and DIC Set-Up

Three bent specimens are subjected to fatigue loading, using a servo-hydraulic fatigue test bench, Zwick Roell HA100, as shown in the left of Fig. 2. Constant amplitude force-controlled tests are performed with a tensile load ratio R of 0.1, a maximum load of 6 kN and at a frequency of 16 Hz. In this case, the minimum load amounts to 10% of the maximum. To monitor the strain evolution of the curved surface inside the bend, a stereo-DIC set-up is used, shown in Fig. 2. The set-up consists of two (Allied Vision) Manta G609 CCD cameras that are fitted with lenses with a focal length of 25 mm.

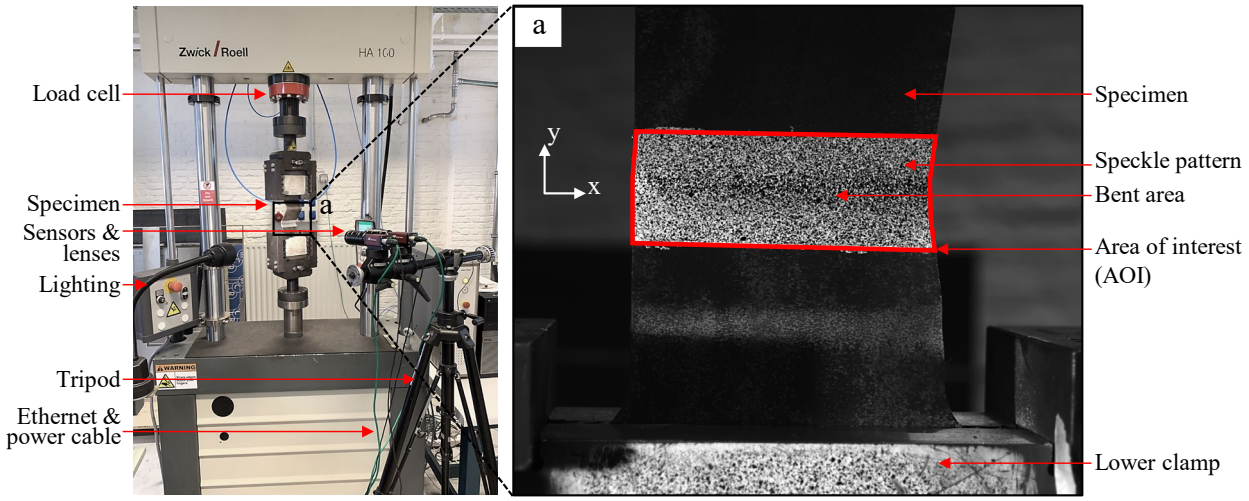

Figure 2 Fatigue testing and DIC set-up. (a) DIC field-of-view of bent area with speckle pattern.

A field-of-view of 230x184 mm^2 was targeted with a stand-off distance of 480 mm, resulting in a mm-to-pixel ratio of 0.08 (mm/px). Optimal DIC settings were obtained for the current set-up through a performance analysis. Further details of the applied settings can be found in Table 2.

Taking into account the average experimental fatigue life N_f^{exp} at the tested load range, a specific image capturing sequence is followed, reported in Table 2. In this way, displacement-fields can be obtained at various stages of fatigue life N_f^{exp}. First, a reference image (0-ref.) is taken at zero load together with another static image (0-noise) to compute and consider the noise level. Subsequently, images at minimum and maximum load are captured at the beginning and ending of every fixed interval of cycles ΔN. Therefore, a cycle limit is consistently entered in the testing software, starting with intervals of 50x10^3 cycles and decreasing to 20x10^3 cycles. Once this limit is exceeded, the load range is applied manually and images are captured, using MatchID Grabber 2020.

Using the processing parameters of Table 3, the images are then correlated and the strain fields computed. Images at the minimum and maximum load allow for plotting the strain range as a function of the amount of fatigue loading cycles. Considering the gradual decrease in dynamic stiffness of the material caused by fatigue loading, a gradually increasing strain range can be expected followed by accelerated strain localisation and growth.

Table 2 Image capturing sequence for monitoring the evolution of the strain field used for bent specimen with r/t=3.

Image	F (kN)	ΔN (x10^3 cycles)	N (x10^3 cycles)	% N_f
0	0-ref.	-	0	0
1	0-noise	-	0	0
2	0.6	-	0	0
3	6	-	0	0
4	0.6	50	50	8
5	6	-	50	8
6	0.6	50	100	16
7	6	-	100	16
8	0.6	40	140	56
9	6	-	140	56
10	0.6	50	190	76
11	6	-	190	76
12	0.6	20	270	96
13	6	-	270	96

Table 3 Experimental and processing parameters of stereo-DIC set-up.

Experimental parameters	Value	Processing parameters	Specification/Value
θ(x) (°)	-0.01	Matching criteria	ZNSSD
ϕ(y) (°)	10.74	Shape function	Affine
ψ(z) (°)	-0.10	Interpolation function	Bicubic splines
T_x (mm)	72.98	Progress history	Spatial
T_y (mm)	0.48	Subset size (SS) (px)	19
T_z (mm)	13.51	Step size (ST) (px)	6
Avg. noise level (%)	0.49	Strain Window (SW)	15
Camera resolution	2752x2206	Strain tensor – Polynomial	Euler-Almansi – Q4
Strain resolution (μm/m)	93.97	Virtual Strain Gauge (VSG) (px)	84

Results

Evolution of strain

To assess the degradation of material during fatigue loading, the y-component of strain is computed and analysed for the bent area of the specimen with a bend ratio of 3, as shown in Fig. 3. The strain fields of six stages of the fatigue test are captured and compared for the maximum load. During the initial load cycle, a relatively small maximum strain of less than $4x10^{-3}$ is found. After 8% of the total fatigue life, the strain distribution reveals a clear red elliptical region of concentrated strain. This distribution remains unchanged at 16% of fatigue life where the peak of maximum strain is located near to the left edge of the bent area, along the x-axis. Just after 50% of fatigue life, the strain concentration starts to intensify and the peak strain shifts towards the right. This shift could be attributed to the effect of the locally hardened region near the initial peak. From 76% up until 96% of fatigue life, the central region of maximum strain expands and values exceed $4x10^{-3}$, implying that crack propagation occurs in this interval. In addition, the peak strain relocates towards the edge of the bend where a visible fatigue crack could be observed.

In Fig. 4, the minimum, maximum and range of strain is plotted against the amount of cycles for three specimens with different bend ratio. The strain values represent the average value of a data-extraction of a central rectangular area that was identical for the three specimens. Here, the strain range is computed as the difference between maximum and minimum strain and can be seen as an important measure for fatigue damage [10]. From Fig. 4 it is clear that the specimen with smallest bend ratio exhibits the highest values for maximum strain and strain range. Further, the beneficial effect of using a larger bend ratio on the fatigue life seems to saturate for bend ratios of 2.5 and 3. Overall, it can be stated that the strain range remains relatively stable until at least 60% of fatigue life. As of that moment, the observed strain concentration causes an increase in maximum strain followed by fatigue micro-crack initiation. The sudden exponential rise can then be linked with crack propagation and subsequent failure.

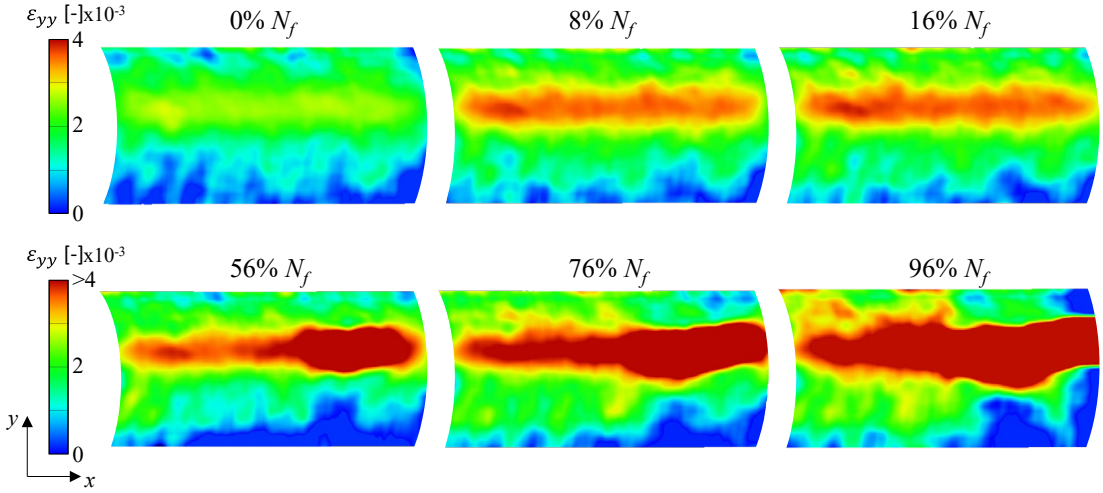

Figure 3 Evolution of the strain fields for specimen with bend ratio of 3.

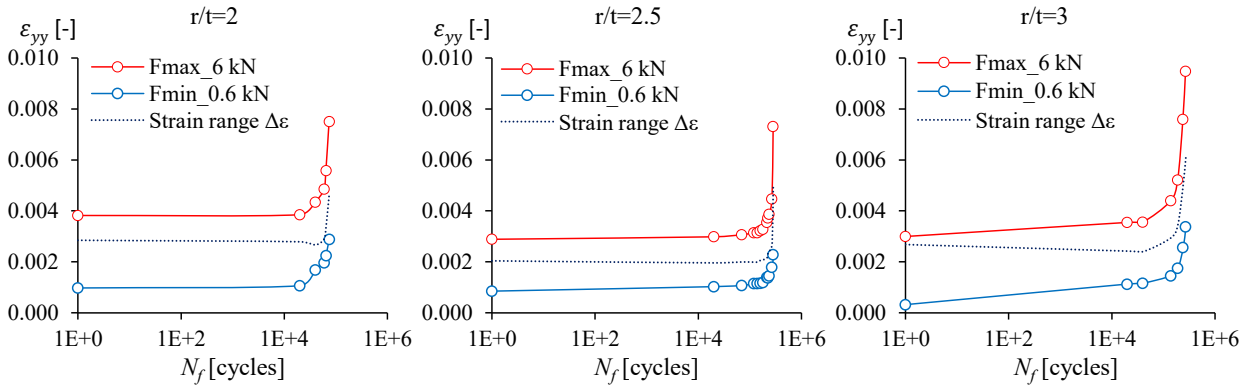

Figure 4 Evolution of the minimum, maximum and range of strain for three bend ratios.

Effect of the Bend Ratio on Strain

To investigate the effect of the bend ratio, the DIC analysis was repeated for three specimens with different bend ratios. In Fig. 5, the strain fields are shown at the initial load cycle and at approximately 75% of fatigue life. A general trend can be observed of increasing strain accumulation for smaller bend ratios. At a later stage of fatigue life, this trend becomes more evident as the average strain in the central region is approximately 22% higher for a bend ratio of 2 ($\overline{\varepsilon_{yy}}$ = 6.43x10^{-3}) relative to a bend ratio of 2.5 ($\overline{\varepsilon_{yy}}$ = 5.26x10^{-3}).

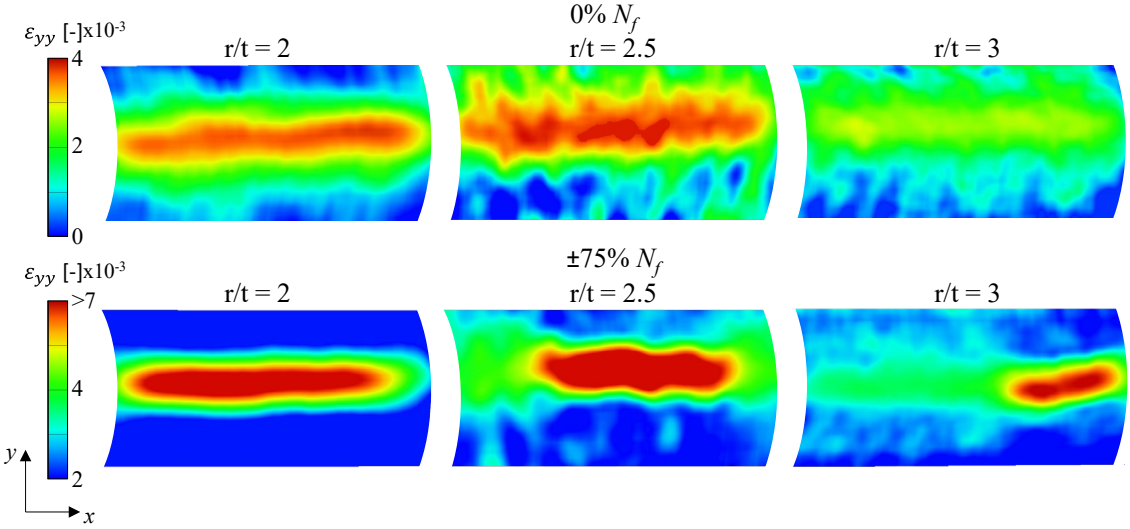

Figure 5 Evolution of strain fields for specimens bent with three different bend ratios.

Microscopic Analysis

A microscopic analysis of one of the specimens was performed to investigate the fracture mechanism of bent HSS. Here, the specimen with a bend ratio of 2 was chosen and the fatigue test was stopped when the measured maximum strain increased exponentially at about 70 000 cycles. The sample was sectioned near the middle of the width of one of the two bends, as illustrated in Fig. 6 (a). This section was then embedded in an epoxy resin followed by polishing up to 1 μm, with a (Beuhler) Phoenix 4000 sample preparation system. Subsequently the sample was etched with Nitric acid for 20 seconds. The microscopic image of Fig. 6 (b) illustrates an initial crack that had reached a length of approximately 0.9 mm. The associated increase in maximum strain means that this crack length coincides with the onset of fatigue propagation for the current specimen and HSS grade. Further, the crack path is almost perfectly straight and orthogonal to the loading direction. Clearly, crack initiation and onset of growth are dominated by a transgranular fracture mode [4]. This observation boils down to the hard and brittle microstructure, consisting of ferrite and tempered martensite that is densely packed due to the large compressive forming strain. Nevertheless, the slightly more ductile ferrite grains can exhibit micro-plasticity, causing slight deviations in the crack path, as noticed in Fig. 6 (c) and (d).

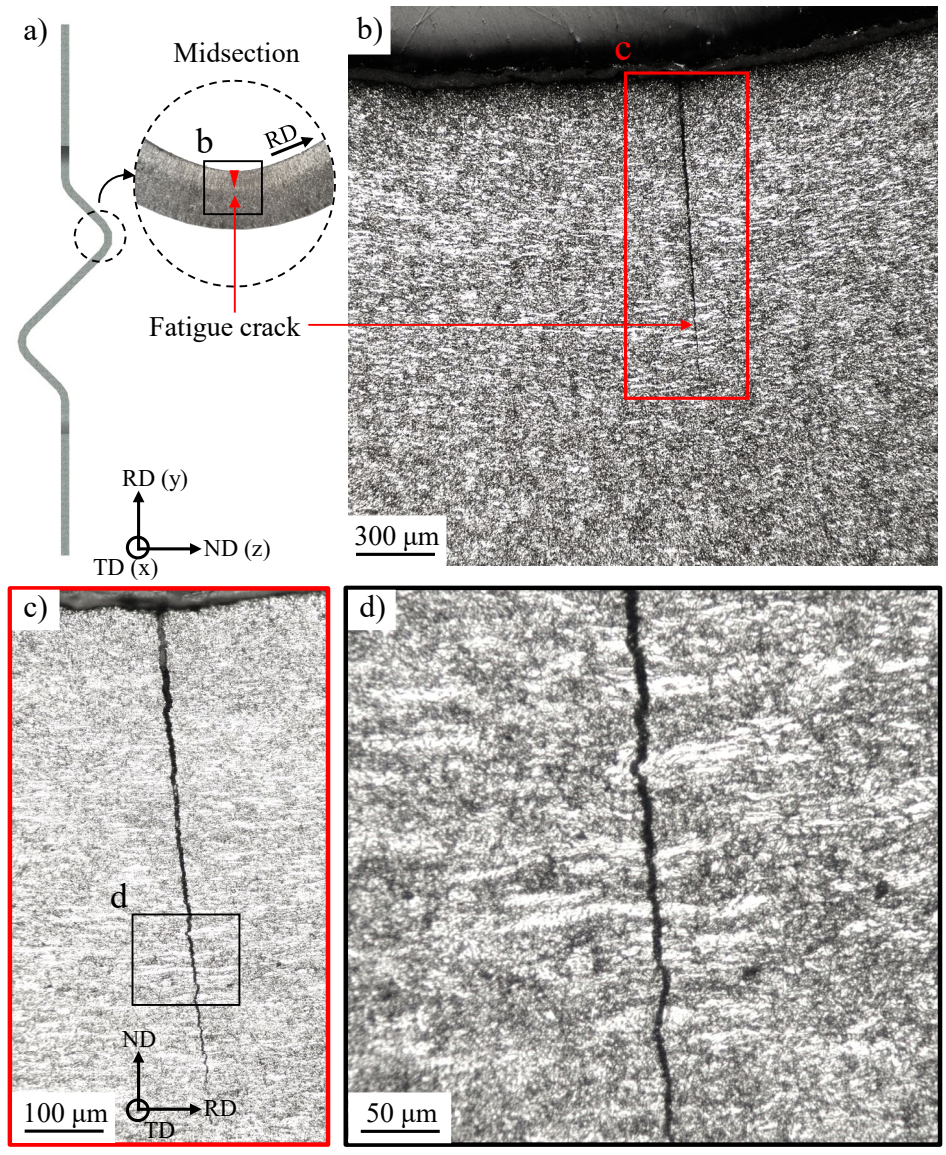

Figure 6 Microscopy of bent specimen with bend ratio of 2: (a) schematic representation of sectioning, (b), (c) and (d) images of the fatigue crack at magnification of x10, x20 and x50 respectively.

This plastic deformation can temporarily lower the growth rate, contributing to a small increase in fatigue resistance. In general, the transgranular fracture mechanism could explain the non-proportional relation between tensile strength and fatigue resistance and must be taken into account for high strength steels that undergo additional strengthening through cold-forming.

Summary

The current paper explores the use of full-field strain measurements for the evaluation of the fatigue performance of a cold-formed HSS specimen. To this end, a specific procedure was proposed to capture the deformation on the inside of the bent area at different stages of fatigue life. A comparison of the strain fields illustrated the stabilisation of strain during the first half of fatigue life with almost no difference in strain distribution. As the load cycles increased, a gradual strain accumulation was noticed that led to rapid localisation and eventual fracture. Further, an improved fatigue resistance was noticed when adopting a larger bend ratio of 2.5 instead of 2. Here, the average strain concentration was found to be at least 22% lower for a bend ratio of 2.5. However, this improvement seemed to saturate for a bend ratio of 3 where a similar fatigue life was obtained. In addition, a microscopic analysis was performed of the specimen with bend ratio of 2. For the given geometry, the onset of crack propagation coincided with a crack length of 0.93 mm. Fatigue crack initiation and propagation were shown to be dominated by a transgranular fracture mode. This was attributed to both the initially hard microstructure accompanied by the microstructural modification caused by forming. These aspects lead to a fracture behaviour that is more brittle than ductile for fatigue and must be taken into account for cold-formed components subjected to cyclic loading.

References

[1] J. Schijve. Fatigue of structures and materials in the 20th century and the state-of-the-art. Int. J. Fatigue 25 (2003) 679–702

[2] R. Talemi, W. De Waele und S. Chhith, Experimental and numerical study on effect of forming process on low-cycle fatigue behaviour, Fatigue Fract. Eng. Mat. Struct. 40 (2017) 2050–2067

[3] B. Vilhauer, C. Bennett, A. B. Matamoros, and S. T. Rolfe. Fatigue behavior of welded connections enhanced with uit and bolting. Technical report. Kansas department of transportation 2008.

[4] R. P. Skelton and D. Gandy. Creep-fatigue damage accumulation and interaction diagram based on metallographic interpretation of mechanisms. Mat. High Temp. 25 (2008) 27–54

[5] K. Denys, S. Coppieters, M. Seefeldt, and D. Debruyne. Investigation into the plastic material behaviour of thick HSS using multi DIC and FEMU. PhD thesis, KU Leuven 2017

[6] V. Vorkov, R. Aerens, D. Vandepitte, and J. Duflou. Experimental investigation of large radius air bending. Int. J. Adv. Manuf. Tech. 92 (2017) 3553–3569

[7] SSAB. Strenx, Hardox and Docol - Bending of high strength steels. Götenborg: Österbergs, 2017.

[8] S. Gothivarekar, C. Jimenez-Pena, S. Coppieters, R. Talemi, and D. Debruyne. Fatigue behaviour and lifetime prediction of cold-formed high strength steel. AIP Conf. Proc. 2113 (2019) 160011–6

[9] S. Gothivarekar, S. Coppieters, R. Talemi, and D. Debruyne. The influence of post-necking strain hardening behaviour on fatigue lifetime prediction of cold-formed high strength steel. Proc. Manuf. 49 (2020) 1250–1256

[10] K. Smith, T. Topper, and P. Watson. A stress-strain function for the fatigue of metals. J. Mater. 5 (1970) 767–778